

# Bridging Hidden States in Vision–Language Models

Benjamin Fein-Ashley  
University of Southern California

Jacob Fein-Ashley  
University of Southern California

## Abstract

*Vision-Language Models (VLMs) are a new family of models that align image content with natural language. Existing approaches typically fuse either (a) early: by mixing tokens/features inside the encoders, or (b) late: by comparing pooled embeddings. Many methods also tie fusion to an autoregressive decoder. However, the hidden states of both modalities already carry rich, modality-specific structure (spatial layout in vision; syntax and semantics in text), so directly aligning these states is a natural way to match what the two modalities “think”. We propose a lightweight fusion module: a few cross-only, bidirectional attention layers placed near the top of both encoders. Each layer projects the vision and text encoder hidden-state sequences into a shared space, attends across modalities, and sends gated residual updates back, with simple stabilizers to improve alignment. The encoders remain non-causal and strong for understanding, while generation stays cleanly decoupled via an optional decoder. Across standard retrieval, VQA, and visual reasoning benchmarks, BRIDGE outperforms comparable VLMs while preserving the bi-encoder efficiency of contrastive models. We make our code publicly available at <https://github.com/jfeinashley/BRIDGE>.*

## 1. Introduction

Vision–Language Models (VLMs) bring visual understanding to Large Language Models (LLMs). Building on advances in language modeling such as GPT-4 [23] and recent multimodal systems (e.g., Gemini [10] and Sonnet 4.5 [2]), interest in scalable multimodal reasoning continues to grow. Most VLMs follow a modular design with three components: a *vision encoder*, a *text encoder*, and a *fusion module* (e.g., [12, 14, 19, 26, 30]). The vision encoder is commonly a transformer (ViT) [11] that captures spatial structure via patches or regions; the text side is a pretrained transformer/LLM. Fusion integrates the two modalities, and an optional decoder (often an LLM) handles generation for captioning or other objectives. VLMs typically adopt one

of two broad fusion strategies:

- **Early fusion:** mixing vision and text tokens/features inside a shared module (e.g., concatenating image patch tokens and word tokens and feeding them into a joint transformer).
- **Late fusion:** encoding vision and text separately, then aligning their pooled embeddings via contrastive or matching losses.

Each approach has trade-offs: early fusion enables tight interactions but may blur unimodal specialization; late fusion preserves strong unimodal backbones but can limit fine-grained cross-modal reasoning [38]. To capture richer interactions beyond contrastive-only alignment, prior work combines contrastive, matching, and captioning objectives [16, 37].

Our method, **BRIDGE**, is a lightweight middle ground that adds a few cross-only, bidirectional attention layers near the top of the vision and text encoders to exchange information in a shared latent space while preserving efficient bi-encoder inference.

This work makes the following contributions:

- We introduce BRIDGE, a lightweight fusion module that inserts cross-only, bidirectional attention layers near the top of vision and text encoders to align full hidden-state sequences in a shared latent space with gated residual updates.
- We propose a simple training recipe that combines standard contrastive and matching objectives with a cycle-consistent cross-attention loss to explicitly encourage stable bidirectional alignment between image and text tokens.
- We show that BRIDGE preserves bi-encoder efficiency for retrieval while improving performance on standard retrieval, VQA, and visual reasoning benchmarks compared to comparable baselines.

## 2. Related Works

### 2.1. Vision-Language Pretraining

Recent advances in VLMs have been propelled by multimodal pretraining. Early approaches in vision-language

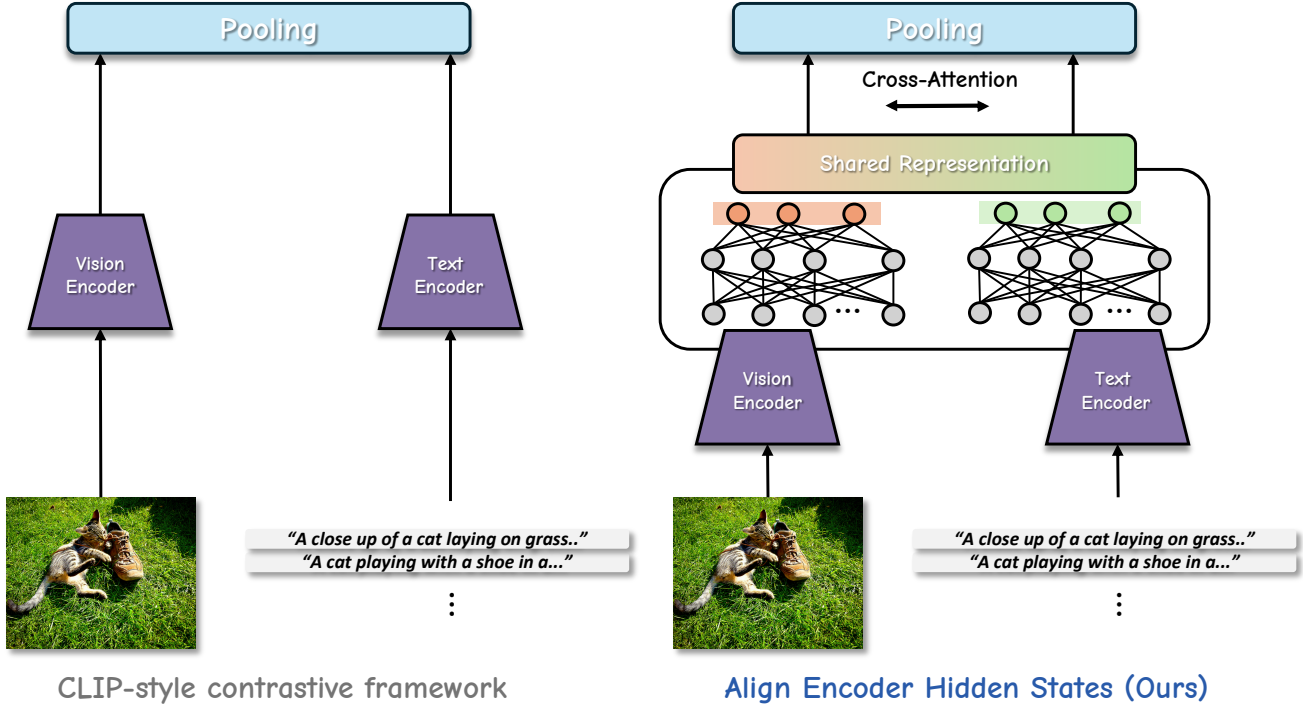


Figure 1. Visual demonstration of BRIDGE alignment space

pretraining models (e.g. LXMERT [30], VisualBERT [19], UNITER [7]) use a transformer-based architecture with cross-attention, relying on pretrained object detectors to fuse image features with text tokens. Foundational contrastive approaches such as CLIP [26] and ALIGN [12] independently encode images and text, aligning pooled embeddings in a shared space. These late-fusion approaches allow for strong zero-shot generalization by aligning text and image embeddings through contrastive learning, but have limited cross-modal reasoning out of distribution [38].

**Multi-Objective Learning.** Many models take an intermediate approach. CoCa [37] unifies contrastive objectives along with captioning. Another approach is cross-attention between modalities. BLIP [17] uses fine tuning with cross-attention to align modalities, while BLIP-2 [18] introduces the querying transformer (Q-former) to bridge the two encoders. ALBEF [16] integrates contrastive and matching objectives along with cross-attention. This combined approach is key for capturing multi-modal interactions.

**MLLMs and Instruction Tuning.** VLMs are often extended to visual question-answering (VQA) and reasoning tasks by adding an LLM as a decoder. Early sys-

tems such as Flamingo [1] and PaLI [6] incorporate cross-attention to integrate image features with language, enabling open-ended visual reasoning. Instruction tuning has emerged as a key strategy for aligning multimodal capabilities. Models such as InstructBLIP [9], LLaVA [22], and MiniGPT-4 [40] fine-tune pretrained VLM backbones using image–text–instruction triplets. More recent instruction-tuned MLLMs, such as Qwen-VL [4], InternVL [8], and Kosmos-2 [24], scale with larger training corpora and more powerful LLM backbones, achieving high performance on VQA tasks. Many models rely on LLM self-attention for alignment, with image and text tokens concatenated and used as the input sequence for the LLM [22, 34]. This constrains token-level grounding and limits detailed bidirectional reasoning between modalities. These limitations motivate architectures that unify scalable LLM reasoning with deeper and more efficient multimodal fusion.

## 2.2. Cross-Modal Representation

Novel alignment methods and representation learning are of interest to overcome these limitations. Query-based alignment, introduced in BLIP-2’s Q-former [18], has been widely adopted. Qwen2-VL uses M-RoPE encoding to improve the fusion of positional information between modalities [31]. Adapter-based fusion has become a very active approach, with models inserting small trainable modules into frozen encoder backbones without the need for full fine-

tuning [29, 33, 36]. Many of these approaches focus on parameter efficient tuning at a small or negligible performance cost. Our approach provides a scalable fusion strategy with a new approach to modality cross-attention. Hidden states of both the text and vision encoder *directly* interact, removing the need for additional adapter stacks. Our architecture allows for scalable overhead and reduces the reliance on LLM self-attention for cross-modal representation in VQA and reasoning tasks.

### 3. Method

We propose **BRIDGE** (bidirectional hidden-state exchange), a framework to directly align hidden states in text and vision encoders for greater multi-modal understanding. This section introduces our model architecture, enumerates learning objectives, and outlines the modular approach for task-specific tuning.

#### 3.1. Model Architecture

Our architecture begins with multi-modal streams entering respective frozen encoders. We apply cross-attention on a select number of interaction layers at the top of each encoder to align their hidden states in a shared space. Interaction layers in the encoders are unfrozen in staged training.

**Encoders.** We employ vision and text encoders. Given image patches and tokenized text, the encoders produce hidden states  $H_t^{(l)}$  and  $H_v^{(l)}$  at each layer  $l$ .

**Hidden State Extraction.**  $H_t^{(l)}$  and  $H_v^{(l)}$  from the encoders are regularized and aggregated with reverse-projected outputs from gating. We use layer normalization and project the hidden states to the interaction layers.

**Interaction layers.** Cross-only multi-head attention (MHA) is applied on the projected hidden states. There is no self-attention; vision only attends to text and text only attends to vision. Text and vision attention are projected to a shared dimension  $d_s$ . After dropout and output projection, outputs are gated with learnable parameters. This provides enhanced modality fusion with adaptive contribution of text and vision, improving stability and performance.

**Downstream Tasks.** InfoNCE loss [26] promotes unimodal representation, allowing for fast retrieval without calculating cross-attention during inference. Optionally, a decoder (an LLM in our case) can be attached after pooling for VQA and reasoning tasks.

**Interaction block (one layer).** Given vision and text hidden states  $H_v^{(l)} \in \mathbb{R}^{N_v \times d_v}$  and  $H_t^{(l)} \in \mathbb{R}^{N_t \times d_t}$ , we first map them to a shared space of width  $d_s$  with PreNorm:

$$Z_v^{(l)} = \text{LN}(H_v^{(l)}) W_{v \rightarrow s}, \quad Z_t^{(l)} = \text{LN}(H_t^{(l)}) W_{t \rightarrow s}. \quad (1)$$

We then apply *cross-only* multi-head attention in both directions (standard dot-product MHA, but with queries from one modality and keys/values from the other):

$$\begin{aligned} A_t^{(l)} &= \text{MHA}_{\text{cross}}(Z_t^{(l)}, Z_v^{(l)}), \\ A_v^{(l)} &= \text{MHA}_{\text{cross}}(Z_v^{(l)}, Z_t^{(l)}). \end{aligned} \quad (2)$$

and update the encoders with a gated residual in their native spaces:

$$\begin{aligned} H_t^{(l+1)} &= H_t^{(l)} + g_t^{(l)} A_t^{(l)} W_{s \rightarrow t}, \\ H_v^{(l+1)} &= H_v^{(l)} + g_v^{(l)} A_v^{(l)} W_{s \rightarrow v}, \end{aligned} \quad (3)$$

where  $g_t^{(l)}, g_v^{(l)} \in (0, 1)$  are learned scalar gates and  $W_{v \rightarrow s}, W_{t \rightarrow s}, W_{s \rightarrow t}, W_{s \rightarrow v}$  are learned projections. We stack  $Q$  such interaction blocks near the top of both encoders.

#### 3.2. Learning Objectives

We jointly optimize standard VLM objectives (image-text contrastive (ITC) loss, masked image/language modeling) and two losses designed to promote cross-modal representation. We utilize a linear combination of losses with learnable scaling parameters

- (1) **Image-Text Matching (ITM) with semi-hard negatives.** ITM loss is used to activate the text encoder. We propose a binary classification task using semi-hard negatives. A small multi-layer perceptron (MLP) on cross-modal embeddings produces a logit indicating contrastive similarity.
- (2) **Cycle-consistent cross-attention.** This objective promotes stable alignment by enforcing cycle-consistent cross-attention.

**Training objective.** From the cross-fused encoders we obtain pooled text and image embeddings  $p_t^{(i)}, p_v^{(i)}$  for each paired example  $i$  in a minibatch of size  $B$ . Following CLIP [26], we use a symmetric InfoNCE image-text contrastive loss with similarities  $S_{ij} = \langle p_t^{(i)}, p_v^{(j)} \rangle / \tau_c$ :

$$\begin{aligned} \mathcal{L}_{\text{itc}} = & -\frac{1}{2B} \sum_{i=1}^B \log \frac{\exp(S_{ii})}{\sum_{j=1}^B \exp(S_{ij})} \\ & -\frac{1}{2B} \sum_{j=1}^B \log \frac{\exp(S_{jj})}{\sum_{i=1}^B \exp(S_{ij})}. \end{aligned} \quad (4)$$

For cycle-consistent cross-attention, we average the per-head attention probabilities from text-to-vision and vision-to-text within each interaction layer to obtain  $\bar{P}_{t \rightarrow v}$  and  $\bar{P}_{v \rightarrow t}$ . The round-trip products

$$C_v = \bar{P}_{t \rightarrow v} \bar{P}_{v \rightarrow t}, \quad C_t = \bar{P}_{v \rightarrow t} \bar{P}_{t \rightarrow v}$$

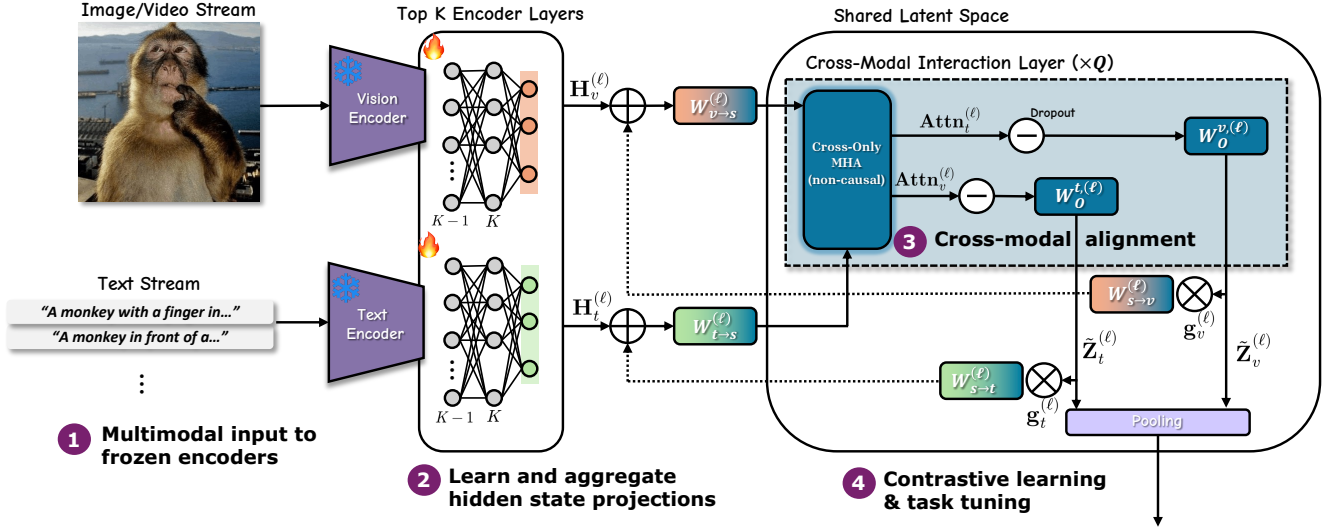


Figure 2. Architecture framework for **BRIDGE**. We propose an architecture where the hidden states of text and vision encoders are aligned directly rather than through pooled embeddings and contrastive loss. In a shared latent space, cross-only MHA is applied with residuals reverse-projected to respective embedding spaces.

are encouraged to be close to identity via a simple diagonal penalty:

$$\mathcal{L}_{\text{cyc}} = -\frac{1}{2} \left( \text{mean} \left( \log \text{diag}(C_v) \right) + \text{mean} \left( \log \text{diag}(C_t) \right) \right). \quad (5)$$

In addition, we use a binary image–text matching loss  $\mathcal{L}_{\text{itm}}$  with semi-hard negatives, and optional masked language/image modeling losses  $\mathcal{L}_{\text{mlm}}$  and  $\mathcal{L}_{\text{mim}}$ . The total objective is a weighted sum of all of the listed loss functions.

### 3.3. Task-Specific Tuning

The proposed framework supports flexible downstream adaptation. For discriminative tasks such as VQA, we fine-tune the cross-fused encoder outputs  $\bar{H}_t$  and  $\bar{H}_v$  with an LLM decoder. For retrieval benchmarks, we use the unimodal projection heads to enable efficient similarity search without cross-attention at inference. The combination of unimodal and cross-modal ITC loss promotes unimodal representation for retrieval.

This modular design allows the model to serve as both a high-capacity vision–language encoder and a foundation for generative multi-modal reasoning tasks, providing a unified architecture for alignment, retrieval, and understanding tasks.

### 3.4. Training Scheme

We find that it is best to train our method in three steps.

**Stage A (stabilize):** freeze both encoders; train only interaction layers, gates, positional biases, and pooled heads.

**Stage B (align):** unfreeze top  $K$  blocks of each encoder (closest to interaction layers).

**Stage C (task tuning):** Involves finetuning for specific tasks. For understanding tasks, attach a classifier head on pooled  $\bar{H}_t/\bar{H}_v$  or token-wise heads on  $\bar{H}_t, \bar{H}_v$ . For retrieval, use  $P_t^u, P_v^u$  for fast bi-encoder search (no extra finetuning needed). For generation, attach a separate causal decoder that cross-attends to frozen vision features or compact bridge latents.

## 4. Experiments

All models and configurations that we display in these experiments portray the maximum limit of our computational budget: that is, we scale the models as much as we can to have a fair comparison. Additionally, we compare against works/models that have a similar parameter size and training/pretraining configuration to exhibit the most “apples-to-apples” comparison that is possible.

### 4.1. Image–Text Retrieval

We evaluate BRIDGE on bidirectional image–text retrieval using the MSCOCO dataset [21] with the standard Karpathy 5K split [13] and the Flickr30K dataset [25]. All models are pretrained on Visual Genome [15], Conceptual Captions [27], and Conceptual 12M [5]. We then fine-tune on the union of the MSCOCO train and restval splits for COCO retrieval, and on the standard train split for Flickr30K.

For each image–caption pair, we optimize the unimodal and cross-modal InfoNCE objectives together with the image–text matching (ITM) loss and the cycle-consistent cross-attention loss introduced in Section 3. At inference

Model	Backbone		# Params	MSCOCO (Karpathy 5K)				Flickr30K (1K test)			
	Image	Text		TR@1	TR@5	IR@1	IR@5	TR@1	TR@5	IR@1	IR@5
CLIP [26]	ViT-B/32	Transformer	151M	37.8	62.4	58.4	81.5	86.5	98.0	67.0	88.9
ALBEF [16]	ViT-B/16	BERT-Base	203M	77.6	94.3	60.7	84.3	77.6	94.1	61.0	84.5
BLIP (14M) [17]	ViT-B/16	BERT-Base	213M	80.6	95.2	63.1	85.3	96.9	99.9	87.5	97.6
<b>BRIDGE (Ours)</b>											
2 interaction layers	ViT-B/16	BERT-Base	236M	81.3	96.3	66.9	86.4	97.2	99.9	88.2	97.8
4 interaction layers	ViT-B/16	BERT-Base	250M	81.5	96.5	67.2	86.7	97.4	99.9	88.5	97.9
6 interaction layers	ViT-B/16	BERT-Base	264M	81.6	96.6	67.5	86.9	97.5	99.9	88.8	98.0

Table 1. **Image–Text Retrieval on MSCOCO and Flickr30K.** Comparison of recent VLMs on the MSCOCO Karpathy 5K split [13] and the Flickr30K 1K test set [25]. TR: text-to-image retrieval; IR: image-to-text retrieval. All values are Recall (%).

time, BRIDGE performs retrieval using only the unimodal projection heads from the text and vision encoders, without running cross-attention, keeping the test-time cost comparable to contrastive models such as CLIP.

We report Recall@K for text-to-image retrieval (TR@1/5) and image-to-text retrieval (IR@1/5), following prior work. As shown in Table 1, BRIDGE consistently improves over CLIP, ALBEF, and BLIP on MSCOCO when using comparable ViT-B/16 and BERT-Base backbones. Increasing the number of interaction layers strengthens cross-modal alignment and yields monotonic gains in both TR and IR performance, with the 6-layer variant achieving the best overall R@1 and R@5 under the same pretraining data. Table 1 also reports results on Flickr30K, demonstrating that the same unimodal retrieval heads generalize to a distinct retrieval benchmark.

## 4.2. Visual Question Answering (VQA)

We further evaluate BRIDGE on open-ended visual question answering using the VQAv2 benchmark [3], which augments MSCOCO images with balanced question-answer pairs to reduce language priors. Following the standard protocol, we train on the official train and validation splits and report single-model performance on the test-dev and test-std splits via the evaluation server.

**Setup.** For VQA, we attach an autoregressive Transformer decoder on top of the cross-fused representations  $\tilde{H}_t$  and  $\tilde{H}_v$  introduced in Section 3. The decoder is initialized from a pretrained LLM and fine-tuned jointly with the interaction layers, while keeping the unimodal encoders frozen except for the selected cross-attention blocks. Questions are tokenized and concatenated with a special [VQA] token, and answers are generated as short text sequences. We follow prior work [7, 16, 17, 20, 32, 39] and restrict the answer space to the most frequent training answers, optimizing a token-level cross-entropy loss over the decoded sequence, i.e., a standard language modeling (LM) loss. In contrast, UNITER [7], OSCAR [20], and VinVL [39]

formulate VQA as answer classification and apply a linear classifier on top of the multimodal [CLS] representation over the same fixed answer set without an autoregressive decoder.

**Baselines.** We compare BRIDGE against strong vision–language pretraining methods spanning both region-based and fully end-to-end architectures. Region-level models such as UNITER [7], OSCAR [20], and VinVL [39] rely on Faster R-CNN features and Transformer-based fusion, while more recent patch-based VLP models including ALBEF [16], BLIP [17], and SimVLM [32] use ViT-style encoders and large-scale weakly supervised pretraining. All baselines are evaluated under their published single-model settings with comparable backbone capacity.

**Results.** Table 2 summarizes VQAv2 performance. Region-based methods achieve strong accuracy but require an external detector, while patch-based models (ALBEF, BLIP, SimVLM) benefit from tighter image–text coupling. BRIDGE builds on a ViT-B/16 image encoder and a BERT-Base text encoder, but differs in that it explicitly aligns hidden states via bidirectional cross-only attention. Across different numbers of interaction layers, BRIDGE provides competitive VQA performance while maintaining the same unimodal encoders used for retrieval in Section 4. Increasing the number of interaction layers generally improves accuracy, reflecting the benefit of deeper cross-modal fusion for compositional reasoning.

## 4.3. Natural Language Visual Reasoning

We evaluate BRIDGE on natural language visual reasoning using the NLVR2 benchmark [28], which requires deciding whether a natural language statement correctly describes a pair of images. We fine-tune a lightweight binary classifier on top of the cross-fused representation from Section 3, reusing the same ViT-B/16 image encoder and BERT-Base text encoder as in our retrieval and VQA experiments.

Model	Backbone		VQAv2 [3]	
	Image	Text	test-dev	test-std
UNITER [7]	Faster R-CNN	BERT-Base	73.8	74.0
OSCAR [20]	Faster R-CNN	BERT-Base	73.6	73.8
VinVL [39]	Faster R-CNN	BERT-Base	76.5	76.6
ALBEF [16]	ViT-B/16	BERT-Base	75.8	76.0
BLIP (14M) [17]	ViT-B/16	BERT-Base	78.3	78.3
SimVLM [32]	Transformer	Transformer	80.0	80.3
BRIDGE (Ours)	ViT-B/16	BERT-Base	<b>80.6</b>	<b>80.7</b>

Table 2. **VQA on VQAv2.** Comparison of BRIDGE with prior vision–language models on the VQAv2 benchmark [3]. All values are overall VQA accuracy (%).

Model	Backbone		NLVR2 [28]	
	Image	Text	dev	test-P
ALBEF (4M) [16]	ViT-B/16	BERT-Base	80.24	80.50
ALBEF (14M) [16]	ViT-B/16	BERT-Base	82.55	83.14
TCL [35]	ViT-B/16	BERT-Base	80.54	81.33
BLIP (14M) [17]	ViT-B/16	BERT-Base	82.67	82.50
BRIDGE (Ours)	ViT-B/16	BERT-Base	<b>83.04</b>	<b>82.87</b>

Table 3. **Natural language visual reasoning on NLVR2.** Accuracy (%) on the NLVR2 dev and public test set (Test-P) for models with ViT-B/16 and BERT-Base backbones.

Table 3 reports accuracy on the NLVR2 dev and public test (Test-P) splits.

## 5. Ablation Studies

To isolate the effect of the bridge architecture itself, we compare BRIDGE to variants that use the same encoders and training data but differ in how (or whether) cross-modal interaction is performed. As shown in Table 5, replacing the bridge with pure late fusion notably degrades performance, while adding even a shallow pooled-only bridge helps. Moving from pooled fusion to hidden-state fusion further improves both TR and IR, and our cross-only interaction design yields the strongest retrieval performance.

To better understand how our model organizes the multi-modal representation space, we visualize the learned embeddings using UMAP (Fig. 3). Each panel shows the 2D projection of paired vision and text embeddings for the baseline (standard embeddings of the frozen ViT and BERT encoders), CLIP, and our BRIDGE model. The baseline produces scattered, partially separated clusters, indicating that the two modalities are not well aligned. CLIP tightens the clusters but still exhibits a clear modality gap: vision and text embeddings occupy distinct regions of the space. In contrast, BRIDGE yields compact, highly overlapping

Loss configuration	MSCOCO (Karpathy 5K)		VQAv2 [3]	
	TR@1	IR@1	test-dev	test-std
<b>Effect of loss components for BRIDGE (ViT-B/16 + BERT-Base)</b>				
InfoNCE only (uni + cross)	79.8	65.0	79.0	79.1
InfoNCE + ITM (no cycle)	80.8	66.4	79.9	80.0
InfoNCE + cycle (no ITM)	80.5	66.2	80.1	80.2
Full model (InfoNCE + ITM + cycle)	<b>81.6</b>	<b>67.5</b>	<b>80.6</b>	<b>80.7</b>

Table 4. **Effect of loss components on MSCOCO retrieval and VQAv2.** Ablation over the loss functions used to train BRIDGE. All variants use the same ViT-B/16 image encoder, BERT-Base text encoder, number of interaction layers  $Q$ , and pretraining data. We report Recall@1 (%) on MSCOCO Karpathy 5K and VQAv2 accuracy (%) on test-dev and test-std.

clusters where vision and text points for the same examples lie close together. This qualitative behavior matches our quantitative results, suggesting that BRIDGE learns a substantially better aligned and more discriminative joint representation than the alternatives.

We next study where to insert the interaction layers within the encoders. Table 6 compares using the bridge only in early, middle, or top layers, as well as a staggered configuration. Placing the interaction layers near the top of both encoders consistently performs best, with the staggered variant performing comparably, suggesting that cross-modal fusion is most effective after strong unimodal features have been formed.

Finally, we ablate the training objectives used for BRIDGE. Table 4 reports MSCOCO retrieval and VQAv2 performance when using only unimodal and cross-modal InfoNCE, adding ITM, adding cycle-consistency, or combining all three. While InfoNCE alone already gives strong results, both ITM and the cycle-consistent cross-attention loss contribute additional gains, and the full loss cocktail yields the best retrieval and VQA accuracy.

## 6. Limitations

While BRIDGE improves cross-modal alignment and achieves SoTA performance on our experiments, our study has several limitations. First, our backbone encoder models are relatively small, and the number of interaction layers is kept small due to computational budget, so our results may underestimate the potential gains at larger scales. Second, we evaluate on a focused set of benchmarks; instruction-tuned MLLMs such as LLaVA and related systems, as well as large contrastive or captioning models like CLIP and BLIP, may still outperform BRIDGE on open-ended dialogue or heavily instruction-following settings where they are specifically optimized. We view BRIDGE as complementary to these approaches, providing a modular fusion mechanism that preserves efficient unimodal inference and can be paired with existing decoders.

Model	Cross-Modal Design		MSCOCO (Karpathy 5K)			
	Interaction Layers	Fusion Type	TR@1	TR@5	IR@1	IR@5
<b>BRIDGE Architecture Ablations (ViT-B/16 + BERT-Base)</b>						
No-Bridge (late fusion)	—	pooled [CLS] only	77.0	94.0	60.0	83.5
Pooled-only bridge	1 cross block	pooled features only	79.5	95.5	63.0	85.0
Hidden-state bridge (self+cross)	$Q$ layers	token-level, self+cross	80.7	96.0	66.0	86.0
BRIDGE (cross-only, ours)	$Q$ layers	token-level, cross-only	<b>81.6</b>	<b>96.6</b>	<b>67.5</b>	<b>86.9</b>

Table 5. **Effect of the bridge architecture on MSCOCO image–text retrieval.** Ablation over the presence and structure of the BRIDGE interaction layers. All variants use the same ViT-B/16 image encoder, BERT-Base text encoder, and pretraining data; we report Recall@K (%) on the Karpathy 5K split.

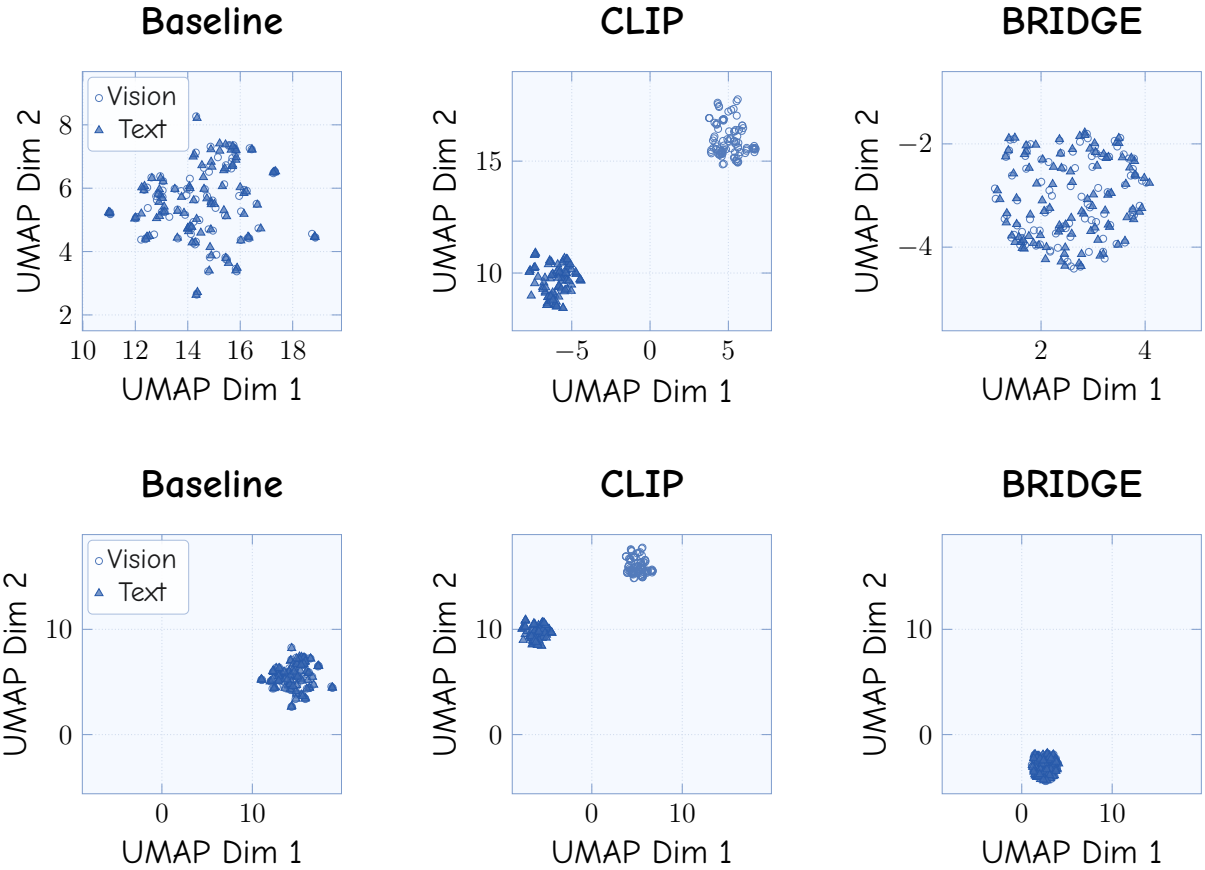


Figure 3. UMAP visualization of the joint vision–text embedding space for the baseline encoders, CLIP, and our BRIDGE model. Points denote individual examples, with markers indicating modality (vision vs. text). The baseline encoders produce diffuse clusters with noticeable separation between modalities, and CLIP, while more compact, still exhibits a clear shift between vision and text regions. BRIDGE instead forms tight, overlapping clusters in which vision and text embeddings for the same examples are nearly co-located, indicating a much smaller modality gap and a more coherent shared representation space. This improved alignment explains the stronger cross-modal retrieval and transfer performance of BRIDGE observed in our experiments. The bottom row contains the same data as the top row, but keeps the axes the same scale.

Model	Interaction Placement		MSCOCO (Karpathy 5K)			
	Text Encoder	Image Encoder	TR@1	TR@5	IR@1	IR@5
<b>Effect of Interaction Layer Placement (ViT-B/16 + BERT-Base)</b>						
Early-only	lowest $Q$ layers	lowest $Q$ layers	80.2	96.0	66.2	86.0
Middle-only	middle $Q$ layers	middle $Q$ layers	81.0	96.3	66.9	86.3
Late-only (top)	highest $Q$ layers	highest $Q$ layers	<b>81.6</b>	<b>96.6</b>	<b>67.5</b>	<b>86.9</b>
Staggered (uniform)	uniformly spaced $Q$ layers	uniformly spaced $Q$ layers	81.4	96.5	67.3	86.7

Table 6. **Effect of interaction-layer placement on MSCOCO image–text retrieval.** Ablation over which encoder layers are selected as cross-modal interaction layers. All variants use the same ViT-B/16 image encoder, BERT-Base text encoder, number of interaction layers  $Q$ , and pretraining data; we report Recall@K (%) on the Karpathy 5K split.

## 7. Conclusion

We introduced BRIDGE, a lightweight fusion module that directly aligns the hidden states of vision and text encoders using a small number of cross-only, bidirectional attention layers. The design of BRIDGE preserves bi-encoder efficiency for retrieval, while also enabling token-level interaction that improves multimodal representation. BRIDGE allows for a simple staged training approach that can be adapted for other VLMs and MLLMs. Across MSCOCO and Flickr30K retrieval, VQAv2, and NLVR2, BRIDGE delivers consistent gains over comparable backbones. Ablations show that hidden-state fusion (rather than pooled-only fusion), late placement of interaction layers, and the full combination of losses are key contributors to performance.

## References

- [1] Jean-Baptiste Alayrac et al. Flamingo: A visual language model for few-shot learning. In *Advances in Neural Information Processing Systems (NeurIPS)*, 2022. [2](#)
- [2] Anthropic. Claude sonnet 4.5 system card. Technical report, Anthropic, 2025. Model card for Claude Sonnet 4.5. [1](#)
- [3] Stanislaw Antol, Aishwarya Agrawal, Jiasen Lu, Margaret Mitchell, Dhruv Batra, C. Lawrence Zitnick, and Devi Parikh. Vqa: Visual question answering. In *International Conference on Computer Vision (ICCV)*, 2015. [5, 6](#)
- [4] Jianwei Bai et al. Qwen-vl: A versatile vision-language model. *arXiv preprint*, 2023. Qwen series vision-language models; public model releases. [2](#)
- [5] Soravit Changpinyo, Piyush Sharma, Nan Ding, and Radu Soricut. Conceptual 12M: Pushing web-scale image-text pre-training to recognize long-tail visual concepts. In *Proceedings of the IEEE/CVF Conference on Computer Vision and Pattern Recognition (CVPR)*, 2021. [4](#)
- [6] Xi Chen et al. Pali: A jointly-scaled multilingual language–image model. In *Proceedings of the International Conference on Learning Representations (ICLR) 2023*, 2022. arXiv preprint arXiv:2209.06794 [cs.CV,cs.CL]. [2](#)
- [7] Yen-Chun Chen et al. Uniter: Universal image-text representation learning. In *ECCV*, 2020. [2, 5, 6](#)
- [8] Zhiwei Chen et al. Internvl: Scaling up vision foundation models and aligning with large language models. *arXiv preprint*, 2023. InternVL project / repo: OpenGVLab. [2](#)
- [9] Wenliang Dai et al. Instructblip: Towards general-purpose vision-language models with instruction tuning. In *Proceedings of the 2023 Conference on Neural Information Processing Systems (NeurIPS) / OpenReview entry*, pages —, 2023. Open-sourced in LAVIS project. [2](#)
- [10] Google DeepMind. Gemini: A family of highly capable multimodal models. Technical report, 2023. [1](#)
- [11] Alexey Dosovitskiy et al. An image is worth 16x16 words: Transformers for image recognition at scale. In *International Conference on Learning Representations (ICLR)*, 2021. [1](#)
- [12] Chao Jia et al. Scaling up visual and vision-language representation learning with noisy text supervision. In *ICML*, 2021. [1, 2](#)
- [13] Andrej Karpathy and Li Fei-Fei. Deep visual-semantic alignments for generating image descriptions. In *Proceedings of the IEEE Conference on Computer Vision and Pattern Recognition (CVPR)*, 2015. [4, 5](#)
- [14] Wonjae Kim, Bokyung Son, and Ildoo Kim. Vilt: Vision-and-language transformer without convolution or region supervision. In *International Conference on Machine Learning (ICML)*, 2021. [1](#)
- [15] Ranjay Krishna, Yuke Zhu, Oliver Groth, Justin Johnson, Kenji Hata, Joshua Kravitz, Stephanie Chen, Yannis Kalantidis, Li-Jia Li, David A. Shamma, Michael S. Bernstein, and Li Fei-Fei. Visual genome: Connecting language and vision using crowdsourced dense image annotations. *International Journal of Computer Vision*, 123(1):32–73, 2017. [4](#)
- [16] Junnan Li et al. Align before fuse: Vision and language representation learning with momentum distillation. In *Neural Information Processing Systems (NeurIPS)*, 2021. [1, 2, 5, 6](#)
- [17] Junnan Li et al. Blip: Bootstrapping language-image pre-training for unified vision-language understanding and generation. In *Proceedings of the 39th International Conference on Machine Learning*, pages 12888–12900. PMLR, 2022. [2, 5, 6](#)
- [18] Junnan Li et al. Blip-2: Bootstrapping language-image pre-training with frozen image encoders and large language models. In *Proceedings of the 40th International Conference on Machine Learning*, pages 19730–19742. PMLR, 2023. [2](#)

[19] Liunian Harold Li et al. Visualbert: A simple and performant baseline for vision and language. In *arXiv preprint arXiv:1908.03557*, 2019. 1, 2

[20] Xiujun Li, Xi Yin, Chunyuan Li, Pengchuan Zhang, Xiaowei Hu, Lei Zhang, Lijuan Wang, Houdong Hu, Li Dong, Furu Wei, Yejin Choi, and Jianfeng Gao. Oscar: Object-semantics aligned pre-training for vision-language tasks. In *Computer Vision – ECCV 2020: 16th European Conference, Glasgow, UK, August 23–28, 2020, Proceedings, Part XXX*, page 121–137, Berlin, Heidelberg, 2020. Springer-Verlag. 5, 6

[21] Tsung-Yi Lin et al. Microsoft coco: Common objects in context. In *European Conference on Computer Vision (ECCV)*, 2014. 4

[22] Haotian Liu et al. Visual instruction tuning. In *Advances in Neural Information Processing Systems 36 (NeurIPS 2023) – Main Conference Track*, pages 34892–34916. Neural Information Processing Systems Foundation, 2023. 2

[23] OpenAI. Gpt-4 technical report. *arXiv preprint arXiv:2303.08774*, 2023. 1

[24] Zhiliang Peng et al. Kosmos-2: Grounding multimodal large language models to the world. *arXiv preprint*, 2023. Grounded MLLM with location tokens and GrIT dataset. 2

[25] Bryan A. Plummer, Liwei Wang, Chris M. Cervantes, Juan C. Caicedo, Julia Hockenmaier, and Svetlana Lazebnik. Flickr30k entities: Collecting region-to-phrase correspondences for richer image-to-sentence models, 2016. 4, 5

[26] Alec Radford et al. Learning transferable visual models from natural language supervision. In *Proceedings of the 38th International Conference on Machine Learning*, pages 8748–8763. PMLR, 2021. 1, 2, 3, 5

[27] Piyush Sharma, Nan Ding, Sebastian Goodman, and Radu Soricut. Conceptual captions: A cleaned, hypernymed, image alt-text dataset for automatic image captioning. In *Proceedings of the 56th Annual Meeting of the Association for Computational Linguistics (ACL)*, 2018. 4

[28] Alane Suhr, Stephanie Zhou, Ally Zhang, Iris Zhang, Huajun Bai, and Yoav Artzi. A corpus for reasoning about natural language grounded in photographs, 2019. 5, 6

[29] Yi-Lin Sung, Jaemin Cho, and Mohit Bansal. Vi-adapter: Parameter-efficient transfer learning for vision-and-language tasks. *arXiv preprint arXiv:2112.06825*, 2021. 3

[30] Hao Tan and Mohit Bansal. Lxmert: Learning cross-modality encoder representations from transformers. In *EMNLP*, 2019. 1, 2

[31] Peng Wang et al. Qwen2-vl: Enhancing vision-language model’s perception of the world at any resolution. *arXiv preprint arXiv:2409.12191*, 2024. 2

[32] Zirui Wang, Jiahui Yu, Adams Wei Yu, Zihang Dai, Yulia Tsvetkov, and Yuan Cao. Simvlm: Simple visual language model pretraining with weak supervision, 2022. 5, 6

[33] Junfei Xiao et al. Palm2-vadAPTER: Progressively aligned language model makes a strong vision-language adapter. *arXiv preprint arXiv:2402.10896*, 2024. PaLM2-VAdAPTER proposes a progressively aligned language model as a strong and efficient vision-language adapter for frozen LLMs. 3

[34] Le Xue et al. Blip-3: A family of open large multimodal models. In *Proceedings of the IEEE/CVF International Conference on Computer Vision (ICCV) Workshops*, pages 6124–6135, 2025. 2

[35] Jinyu Yang, Jiali Duan, Son Tran, Yi Xu, Sampath Chanda, Liqun Chen, Belinda Zeng, Trishul Chilimbi, and Junzhou Huang. Vision-language pre-training with triple contrastive learning, 2022. 6

[36] Juncheng Yang et al. Cross-modal adapter: Parameter-efficient transfer learning approach for vision-language models. *arXiv preprint arXiv:2404.12588*, 2024. 3

[37] Jiahui Yu et al. Coca: Contrastive captioners are image-text foundation models. In *IEEE/CVF Conference on Computer Vision and Pattern Recognition (CVPR)*, 2023. 1, 2

[38] Mert Yuksekgonul et al. When and why vision-language models behave like bags-of-words, and what to do about it? In *Proceedings of the 11th International Conference on Learning Representations (ICLR 2023)*, 2023. 1, 2

[39] Pengchuan Zhang, Xiujun Li, Xiaowei Hu, Jianwei Yang, Lei Zhang, Lijuan Wang, Yejin Choi, and Jianfeng Gao. Vinvl: Revisiting visual representations in vision-language models. In *Proceedings of the IEEE/CVF Conference on Computer Vision and Pattern Recognition (CVPR)*, pages 5579–5588, 2021. 5, 6

[40] Zhengyang Zhu, Pengchuan Zhang, Hangbo Bao, et al. Minigpt-4: Enhancing vision-language understanding with advanced llms. *arXiv preprint arXiv:2304.10592*, 2023. Aligns a frozen visual encoder to a frozen LLM with a projection layer. 2